



A novel sputtered Pd mesh architecture as an advanced electrocatalyst for highly efficient hydrogen production



Antonio de Lucas-Consuegra ^{a,*}, Ana R. de la Osa ^a, Ana B. Calcerrada ^a, José J. Linares ^b, David Horwat ^{c,**}

^a Departamento de Ingeniería Química, Facultad de Ciencias y Tecnologías Químicas, Universidad de Castilla-La Mancha, Ciudad Real, Spain

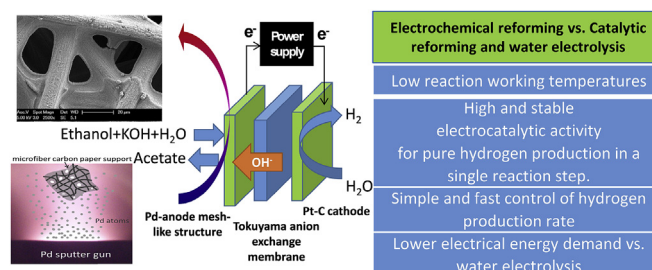
^b Instituto de Química, Universidade de Brasília, Campus Universitário Darcy Ribeiro CP 4478, 70910-900 Brasília, Distrito Federal, Brazil

^c Institut Jean Lamour, UMR7198, Université de Lorraine, F-54011 Nancy, France

HIGHLIGHTS

- AEM electrochemical reforming of ethanol was developed for pure H₂ production.
- A novel sputtered Pd mesh-like anode was used as an advanced electrocatalyst.
- Large H₂ production rates were obtained with low energy requirement.
- The system was stable for long working times.
- Potassium acetate was the main anodic product.

GRAPHICAL ABSTRACT



ARTICLE INFO

Article history:

Received 1 September 2015

Received in revised form

27 April 2016

Accepted 2 May 2016

Available online 9 May 2016

Keywords:

Hydrogen production
Electrochemical reforming
Pd sputtering
Electrolysis
AEM

ABSTRACT

This study reports the preparation, characterization and testing of a sputtered Pd mesh-like anode as an advanced electrocatalyst for H₂ production from alkaline ethanol solutions in an Alkaline Membrane Electrolyzer (AEM). Pd anodic catalyst is prepared by magnetron sputtering technique onto a microfiber carbon paper support. Scanning Electron Microscopy images reveal that the used preparation technique enables to cover the surface of the carbon microfibers exposed to the Pd target, leading to a continuous network that also maintains part of the original carbon paper macroporosity. Such novel anodic architecture (organic binder free) presents an excellent electro-chemical performance, with a maximum current density of 700 mA cm⁻² at 1.3 V, and, concomitantly, a large H₂ production rate with low energy requirement compared to water electrolysis. Potassium hydroxide emerges as the best electrolyte, whereas temperature exerts the expected promotional effect up to 90 °C. On the other hand, a 1 mol L⁻¹ ethanol solution is enough to guarantee an efficient fuel supply without any mass transfer limitation. The proposed system also demonstrates to remain stable over 150 h of operation along five consecutive cycles, producing highly pure H₂ (99.999%) at the cathode and potassium acetate as the main anodic product.

© 2016 Elsevier B.V. All rights reserved.

1. Introduction

The need to expand the supply of domestically produced energy is a strategic issue because fossil fuels, the main energy source, are often imported. In such a domestic production scenario, hydrogen

* Corresponding author.

** Corresponding author.

E-mail addresses: Antonio.lconsuegra@uclm.es (A. de Lucas-Consuegra), david.horwat@univ-lorraine.fr (D. Horwat).

is considered to be an excellent energy carrier for renewable and sustainable-based energy systems via fuel cells utilization [1]. Traditional large-scale production of hydrogen is mainly based on methane reforming process. However, this pathway produces other carbon-derived products such as carbon monoxide and carbon dioxide, together with hydrogen, which requires several reaction and purification steps in order to clean the reformer gas stream before entering the fuel cell. In this sense, there is a growing interest in developing effective alternatives to produce hydrogen, especially for on-site applications by more simple and compact production processes [2]. In this sense, the electrolysis process has gained much attention due to the production of pure hydrogen at high rates in a single reaction step. Thus, a lot of scientific interest has been focused on water electrolysis due to its advantages for the production of clean hydrogen [3]. However, although water electrolysis is a well-established commercial technology, its practical application is limited by the electrical energy consumption due to the high overvoltage required for producing large amounts of hydrogen.

In the last years, the electrolysis of alcohols has demonstrated to be a promising alternative to decrease the energy demand ascribed to the electrolytic production of hydrogen [4]. The high energy contained in these fuels supplies part of the energy requirements, thus reducing the external energy demands, and enables obtaining higher current density values at lower anode potential (below 1.3 V) than required for water electrolysis. In this way, it is possible to produce H_2 with a lower electrical energy requirement (as shown later on, 30 kWh kg H_2^{-1} after deactivation) in comparison with commercial PEM water electrolyzer stacks (50 kWh kg H_2^{-1}) [5]. This process of water alcohols mixture electrolysis has been also named Electrochemical Reforming or Electro-Reforming, and is based on the use of electrical power to split water molecule and transform it into H_2 by the electro-oxidation of the alcohol fuel.

Previous works have already demonstrated the interest of this technique for the production of high purity hydrogen by electrochemical reforming of methanol [4,6–8], glycerol [9–11], ethanol [5,12], bioethanol [13,14] and ethylene glycol [15]. However, most of these previous works have been carried out in Proton Exchange Membrane (PEM) cells and, hence, expensive anodic catalyst typically based on Pt-Ru/C of high metal loadings have been used. Possible utilization of alkaline environment presents the advantage of improved electro-oxidation kinetics with non-precious metal catalysts. In this sense, a previous communication of Chen et al. [14] has demonstrated the interest of using Pd nanoparticles deposited on titania nanotubes for alkaline electrochemical reforming of ethanol, ethylene glycol, glycerol and 1,2-propanediol using an Anion Exchange Membrane (AEM) based electrolysis cell. The authors report polarization curves recorded at 10 mV s⁻¹, showing high electro-catalytic activity for H_2 production, comparable with that of conventional PEM water electrolysis. However, further experiments should be performed in order to address several technological demands, especially the level of purity of the produced H_2 , sub-products formation, influence of the main operation conditions, system durability and anodic catalyst stability under such alkaline conditions.

This study presents, for the first time in literature, the preparation, characterization and testing of a self-standing sputtered Pd mesh-like anode structure of high electro-catalytic activity and stability for alkaline electro-chemical reforming of ethanol-water solutions in alkaline media. Synthesis of self-standing metallic membranes generally involves the conformal deposition of a metal layer on a support followed by local dissolution of the support. This approach has been successfully employed to produce microporous Pd/Au alloy membranes using sputtering as a metal deposition method [16]. The strategy reported in this work is radically

different as it involves the self-formation of a metallic mesh-like structure during deposition on a carbon paper with the carbon microfibers acting as anchorage lines for the Pd mesh-like structure. For that purpose, magnetron sputtering method has been used since it can be easily scaled-up. Moreover, porous films can be produced for conditions associated to a low mobility of the ad-atoms [17], which qualifies it for the synthesis of metal catalysts of large developed surface area. Compared to supported catalysts, self-supported ones offer the possibility to maximize the surface in contact with the reactive medium and, thereby, represent an interesting possibility to improve the electro-catalytic efficiency.

2. Experimental

2.1. Synthesis and characterization of the anodic Pd mesh-like architecture

Magnetron sputtering was used to produce macroporous Pd mesh-like structure by deposition on a microfiber Carbon Paper (Fuel Cell Earth) substrate. A 2" diameter Pd target positioned at a target–substrate distance of 70 mm was sputtered in a pure Argon atmosphere of 11 Pa using a discharge current of 0.3 A. The target was placed off-axis relative to the rotating substrate-holder axis, which enables ensuring a good lateral homogeneity of the flux of deposited material [18]. The overall film density was calculated by weighing the carbon microfiber paper before and after deposition, and measuring the film thickness obtained by deposition on a glass slide. The mass of Pd supported on the carbon paper was also measured before and after experiments by Atomic Absorption Spectrophotometry on a SPECTRA 220FS analyzer. The Pd film structure was also characterized before and after electrocatalytic experiments by X-Ray Diffraction (XRD) analysis using a Philips PW-1710 instrument with Cu K α radiation ($\lambda = 1.5404 \text{ \AA}$). Surface morphology was imaged with a Scanning Electron Microscope (SEM) Philipps XL30S FEG equipped with a field emission gun using an acceleration voltage of 15 kV and through lens detector. Chemical analysis was performed via an Energy-Dispersive Spectrometer (EDS) coupled to the SEM apparatus.

2.2. Preparation of the membrane electrode assembly (MEA)

The prepared sputtered Pd mesh-like structure was used as anode, while standard Pt supported on carbon (20 wt % Pt/C- Alfa Aesar) was adopted as cathode catalyst in the electrochemical reforming unit. Both electrodes were deposited on Carbon Paper substrates (Fuel Cell Earth) with a metal loading of 1.93 mg cm⁻² (measured by Atomic Absorption Spectrophotometry) for the anode and 0.5 mg cm⁻² for the cathode. Geometric surface area was 6.25 cm². Membrane electrode assembly (MEA) was prepared by pressing together anode (Pd), cathode (Pt/C) and a Tokuyama A901 Alkaline Exchange Membrane, applying a load of 1 ton at 120 °C for 3 min. Prior to use, the AEM was pretreated by successive immersion in boiling deionized water for 1 h, and subsequently in 1 mol L⁻¹ KOH for 24 h.

2.3. Electrochemical reforming activity measurements

Experimental tests were carried out in an electrolysis unit described in detail elsewhere [5]. The MEA was introduced between two Teflon gaskets to ensure sealing between anode and cathode compartments (0.2608 cm³ per chamber). Graphitic bipolar plates of 2 cm thickness and 36 cm² area were placed on both sides of the MEA. Parallel grooves were drilled in the graphite plates, with a total surface area of 6.25 cm², which served as flow channels. All the above items were finally placed between two

external Teflon plates, covered with metallic end plates, and were uniformly tightened with nuts and bolts using an electronic torque wrench in order to ensure mechanical stability. The cell had provisions for heating and temperature control.

Electrochemical measurements were carried out in an Autolab potentiostat/galvanostat (PGSTAT30-ECOCHÉMIE) controlled by a Research Electrochemistry software. The anodic compartment of the cell was fed with an aqueous fuel solution (1 mol L^{-1} KOH or NaOH and $0.5\text{--}4 \text{ mol L}^{-1}$ of ethanol solution) at a flow rate of 100 ml min^{-1} using a peristaltic pump. The cathode chamber was supplied with water by a high-pressure liquid pump (HPLP-GILSOM 307) at a constant 1 ml min^{-1} flow rate. The produced hydrogen was assessed with a high-precision flowmeter. Both feeding solutions were preheated at a temperature close to that of the cell, which was always kept in a temperature range between 70 and 90°C . The operation mode was discontinuous, i.e., recirculating both streams to the feed reservoirs, whose volumes were 1 and 0.5 L for the anode and cathode chambers. A scheme of the experimental setup is shown in the Supporting Information (Fig. A1). Two kinds of electrocatalytic experiments were performed: linear voltammetry measurements, at a scan rate of 5 mV s^{-1} , up to a maximum applied potential of 1.3 V and, mild-term reaction experiments of 150 h of duration for a stability study, at a constant current of 1 A (160 mA cm^{-2}). For this latter experiment, the anodic liquid solution was renewed every 35 h.

Analysis of the liquid anodic and gaseous cathodic products were carried out using a high performance liquid chromatography HPLC (Agilent 1100 series) and a gas chromatograph (Bruker 450-GC) coupled online to the gas line, respectively. Total Organic and Inorganic Carbon concentrations were also monitored for the anodic stream using a Multi N/C 3100 Analytik Jena analyzer. For the analysis of the anodic chamber stream, a sample of the solution was collected for 8 and 24 h in order to evaluate the anodic product distribution. The rate of hydrogen production during the electrochemical reforming experiments was also followed by gas-volume measurements, and crosschecked via Faraday's Law calculations, based on the cell current.

3. Results and discussion

3.1. Pd anode characterization

In order to confirm the actual deposition of metallic palladium on the carbon microfibers, EDS analysis has been performed. Fig. 1a shows the EDS spectrum of the sputtered Pd anodic catalyst. Signal is highly dominated by the carbon and palladium X-ray emissions. Traces of oxygen are also detected, which might be associated to minor amounts of surface palladium oxide. Fig. 1b displays the diffractogram of the electrode. The classical Pd face-centered cubic (fcc) crystalline structure can be observed. The presence of two peaks at approximately 26 and 54° associated to the (002) and (004) crystalline arrangements of the graphitic carbon support are due to the low thickness of the Pd thin film in contrast with the higher depth penetration of the X-ray (which is in the order of $10 \mu\text{m}$). Average size of the Pd crystallites has been evaluated to be 14 nm by applying Scherrer formula to the FWHM of the Pd (111) diffraction peak.

In order to visualize the microstructure of the palladium anode, Fig. 2 shows several SEM images of the electrode. Fig. 2a–c clearly confirm that the sputter-deposition process enables the coverage of area of the carbon microfibers exposed to the sputtered flux, which is typical for physical vapor deposition methods based on the condensation of neutral atoms. Furthermore, Fig. 2a and b reveal the continuity and homogeneity of the formed Pd catalyst interconnected over the whole covered carbon paper surface area. Such

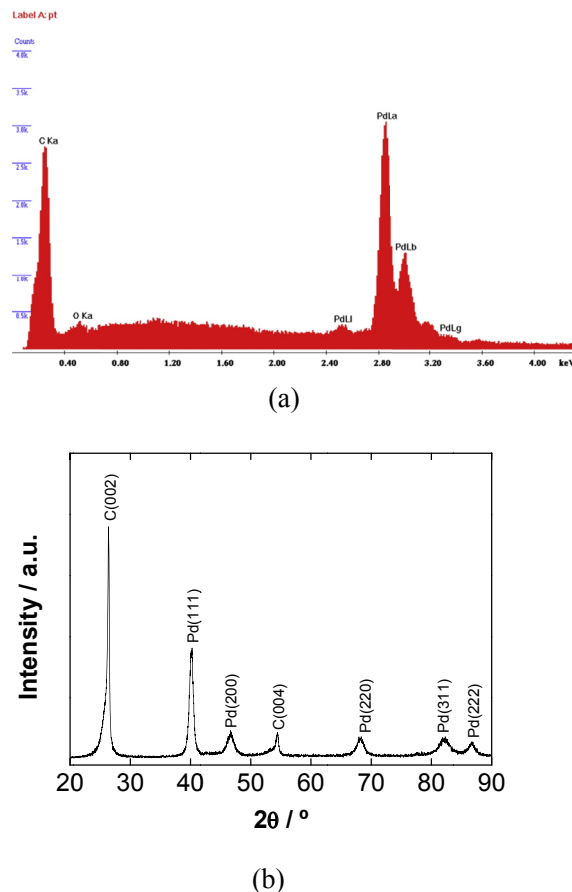


Fig. 1. (a) EDS analysis; and (b) X-Ray diffractogram of the Pd-sputter mesh-like anode.

characteristic is crucial in order to guarantee the continuity in the electronic conduction and, thus, maximize the three-phase-boundary catalyst/ionic carrier/electronic conductor. Pd catalyst expands laterally away from the carbon fibers, forming a self-standing macroscopically porous membrane with most of its surface accessible to the reactive medium. Furthermore, presence of macropores between the fibers may eventually result beneficial for mass transport processes. This structure is an indication of the self-formation of the net-like architecture involving the minimization of the surface energy (further information about this can be found in the Supporting Information, Fig. A2).

Further details of the Pd sputtered anode surface morphology (Fig. 2d and e) show the presence of interconnected porosities shaping the contour of the typical microstructure of hierarchically highly porous films obtained by sputtering under low ad-atom mobility [19,20]: bundles of vertically aligned nanofibers, which domed tops are visible on Fig. 2e, and groups of bundles building up columns, which cross-section is represented by the widest closed “cracks”. Overall degree of porosity has been estimated close to 30%. A cross-section of the Pd sputtered anode is presented in Fig. 2f after fracturing the carbon paper. A columnar microstructure can be seen with penetration of the pores throughout the Pd layer. The latter point is confirmed by the presence of interconnected pores emerging at the backside of the net structure. It can be also observed a good adhesion of the Pd mesh to the carbon substrate with no binder or ionomer adhesion in contrast to conventional anodic catalyst preparation [5,7,13,15].

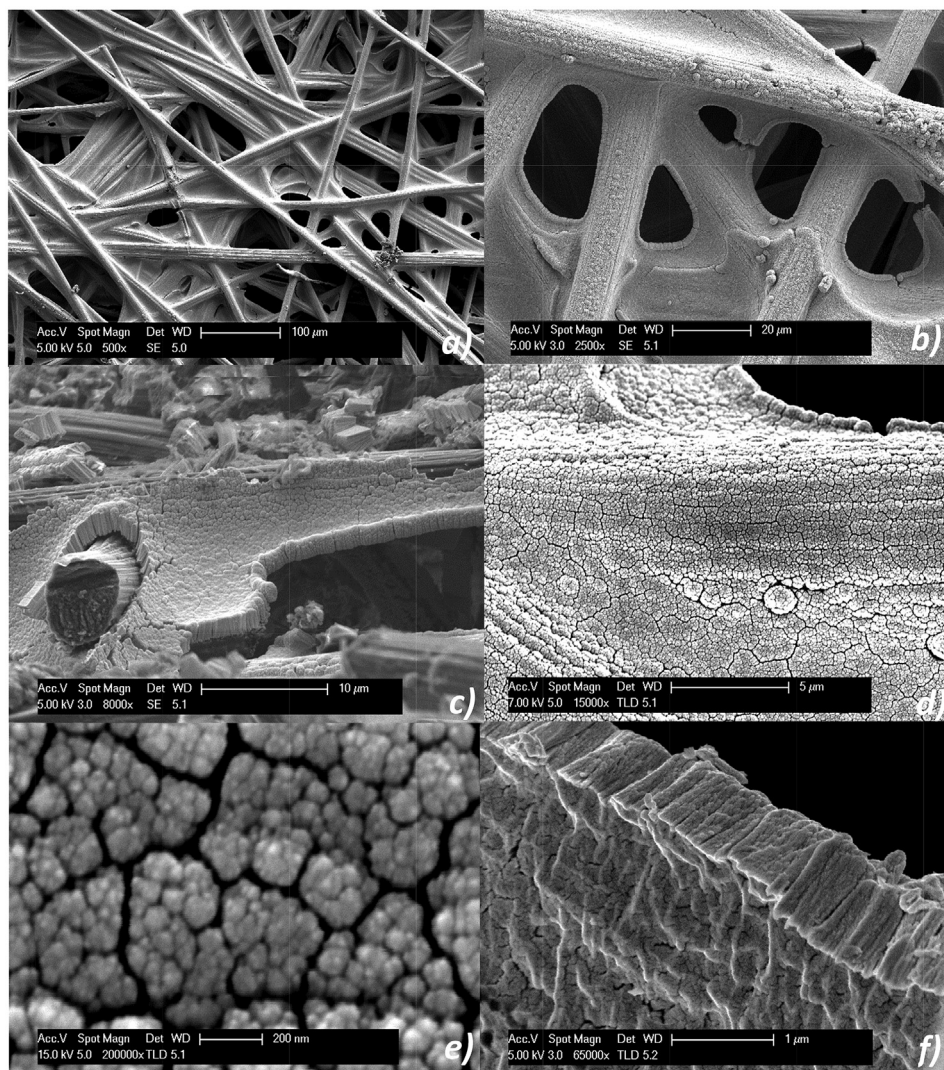


Fig. 2. SEM images of the Pd-sputter mesh-like anode.

3.2. Electrochemical reforming experiments for H_2 production. Preliminary experiments

In order to preliminary demonstrate the viability of alkaline electrochemical reforming of an ethanol solution over the prepared Pd-based anode catalyst, a linear voltammetry experiment was carried out at a constant temperature of $80\text{ }^{\circ}\text{C}$ and scan rate of 5 mV s^{-1} . Fig. 3a illustrates the variation of current density with applied potential ($0\text{--}1.3\text{ V}$ range) for a 2 mol L^{-1} ethanol solution in presence of 1 mol L^{-1} KOH and for 1 mol L^{-1} KOH (free-ethanol solution). Before discussing this result, it is important to note that no current was detected when KOH/water was fed to the anode. As seen, ethanol electrolysis begins at a cell potential above 0.5 V with a continuous linear increase in the current density up to 1.3 V . At this potential, a maximum current density of approximately 600 mA cm^{-2} can be drawn from the system. At such upper limit potential alkaline water electrolysis begins to efficiently operate [21], corroborating that alcohol electrolysis is indeed an opportunity for energy saving compared to water electrolysis. Finally, no apparent mass transfer limitations appeared in the polarization curve. This behavior is noteworthy since one of the main limitations of alkaline alcohol electro-oxidation processes in actual single cell electrodes (thin catalytic layer deposited on the diffusion layer) is

mass transportation associated to the higher viscosity of alkaline solutions, compared to the aqueous ones, and the generation of inorganic salts on the catalytic surface [22]. Macroporosity observed in the sputtered Pd electrode appears to be effective for reducing those issues, thus minimizing mass transfer limitations. Fig. 3b shows the variation of the produced H_2 rate (normalized to STP conditions, at $\text{EtOH } 2\text{ mol L}^{-1}$ and $\text{KOH } 1\text{ mol L}^{-1}$), experimentally determined via volumetric hydrogen flow measurements, vs. the applied current for the same voltammetry experiment. In addition, this figure shows the fitting of the experimental points to the theoretical faradaic H_2 production rate. Fig. 3b reveals that an increase in the current density leads to higher H_2 production rates, which values well fit those predicted by Faraday's law.

Obtained results are similar to those reported in previous studies for alkaline ethanol, glycerol, 1,2-propandiol and ethylene glycol electro-reforming over Pt or Pd/titania nanotubes anodes, in a wide range of reaction conditions [14,23]. Interestingly, current density values obtained in this work are three times higher than the best of those reported for PEM electrochemical reforming of ethanol-water and glycerol-water solutions [24–26] and of the same order than the ones reported previously by Chen et al. [14], using Pd/titania nanotubes AEM electrolyzer. Such a high electro-catalytic performance can be attributed to the particular sputtered

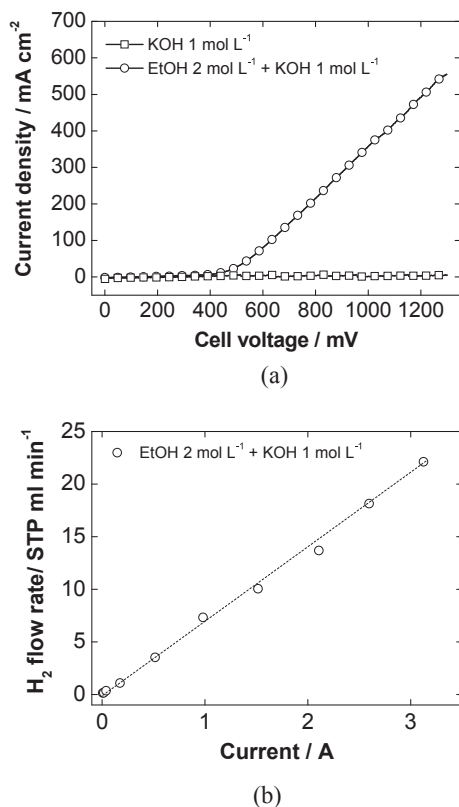


Fig. 3. (a) Polarization curves of alkaline ethanol electro-reforming; (b) Hydrogen production rate for the different currents (straight line represents predicted hydrogen rate by Faraday's law).

Pd microstructure. Most of the palladium is deposited on the uppermost layer of the carbon paper forming an interconnected network of large developed surface area (Fig. 2). This way it is mostly in contact with anionic membrane, carbon paper and liquid electrolyte, maximizing the three-phase boundary layer and, consequently, the electrochemical performance. Furthermore, this particular microstructure allows an efficient transport of fuel/electrolyte (OH^- species are required in the ethanol electro-oxidation) and electro-generated products, in addition to the intrinsic good ethanol electro-oxidation activity of palladium in alkaline medium [27,28]. In addition, for comparison purposes with a reference Pt electrode prepared by the same sputtering conditions, further experiments have been performed in a three electrode electrochemical glass cell (half-cell) (as shown on Fig. A3 of the supporting information material). As can be observed on Fig. A4 (supporting information), the obtained results corroborate the excellent performance of Pd, above that of reference Pt.

3.3. Influence of the operating conditions

Based on good preliminary results, the study was continued with the analysis of the influence of relevant operating conditions, such as the alkali used in the fuel formulation, cell temperature and fuel concentration. Fig. 4 shows polarization curves obtained with 1 mol L⁻¹ NaOH and 1 mol L⁻¹ KOH electrolytes carried out at 80 °C and a 0.5 mol L⁻¹ ethanol solution. Polarization curves evidence that KOH is a more suitable electrolyte for alkaline ethanol electrolysis than NaOH, especially at high current density (high cell voltages > 0.8 V) when the fuel demand is higher. It has been widely observed for hydrogen oxidation, oxygen reduction,

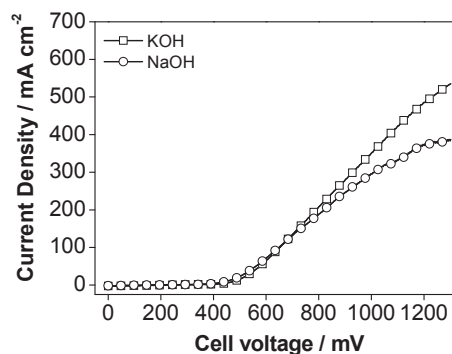


Fig. 4. Influence of the alkali used in the fuel on the performance of the ethanol electroreforming cell (temperature of 80 °C for a 2 mol L⁻¹ ethanol and 1 mol L⁻¹ alkali concentration).

methanol, ethylene glycol and glycerol oxidation and hydrogen peroxide reduction/oxidation over Pt, and to a lower extent, on Au [23,29–33]. The observed differences were explained in terms of non-covalent interactions between hydrated cations $\text{OH}_{\text{ad}}\text{-M}^+(\text{H}_2\text{O})_x$ ($\text{M} = \text{Na}$ or K) and OH_{ad} on Pt/Au. Extrapolating this to the case of Pd, it may be inferred that the lower the size of the alkali metal, the higher the hydration energy and the most favorable formation of that species on the Pd surface. It leads to a reduction of the number of available active sites, which is especially detrimental at high current densities where fuel demand reaches its maximum. Based on the experimental results, it seems that Pd also undergoes a similar deactivation surface phenomenon, more intense in case of the smallest $\text{Na}^+(\text{H}_2\text{O})_x$ cation. On this basis, KOH was selected as the ionic electrolyte for subsequent electrochemical reforming experiments.

Fig. 5 illustrates the influence of temperature and ethanol concentration on the electrochemical reforming process. Polarization curves at 70, 80 and 90 °C are presented in Fig. 5a for a 2 mol L⁻¹ ethanol concentration (electrolyte concentration 1 mol L⁻¹ KOH). As expected, an increase in the temperature leads to higher current densities for the same cell voltages, which is very interesting from a practical point of view, due to larger hydrogen production rates. These results can be explained in terms of higher activity of ethanol electrooxidation and water reduction reactions, larger membrane conductivity and enhanced mass diffusion achieved at higher temperatures [34]. From these results, it is also possible to estimate the activation energy (Table 1) from an Arrhenius plot of the current density at a fixed potential (Fig. 5b). Three different calculations have been done at 600, 700, 800 and 1000 mV in order to observe the evolution of the apparent activation energy with the cell potential. Activation energy is estimated from Eq. (1) [35], where j is the current density in $\text{mA}\cdot\text{cm}^{-2}$, T is the temperature in K, R is the universal gas constant and E_a is the apparent activation energy.

$$E_a = -R \frac{\partial(\ln j)}{\partial(1/T)} \quad (1)$$

The obtained activation energies vary from 13.9 kJ mol⁻¹ to 17.9 kJ mol⁻¹ when the potential is increased from 600 to 1000 mV. Assuming that the obtained activation energy mainly comes from ethanol electrooxidation rather than water reduction, due to the low overvoltage of Pt towards the hydrogen evolution reaction [36,37], the obtained values are within the range presented in the literature. Those range from 8–10 kJ mol⁻¹ [38,39] to larger values between 25 [35,40,41] and 40 kJ mol⁻¹ [42], which discrepancies are most

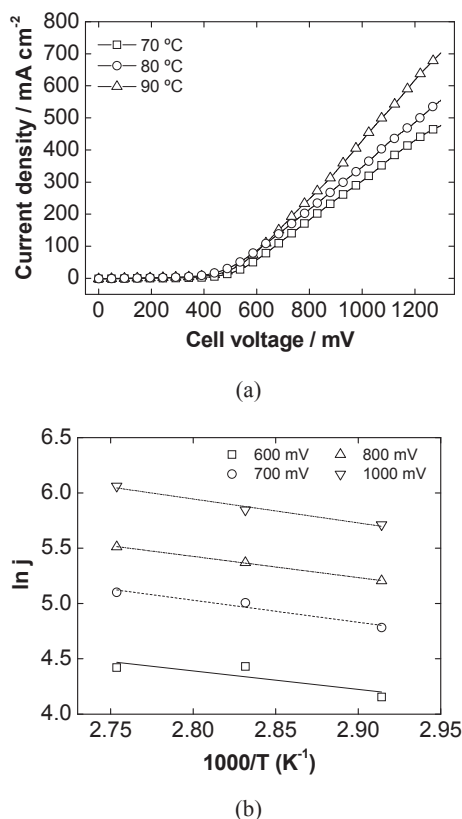


Fig. 5. Influence of: (a) the cell temperature (2 mol L⁻¹ ethanol and 1 mol L⁻¹ KOH fuel composition); and (b) Arrhenius plot for the estimation of the activation energy for this system.

Table 1

Activation energy values of the alkaline ethanol electrolysis process (obtained for a 2 mol L⁻¹ ethanol + 1 mol L⁻¹ KOH fuel composition).

Cell potential/mV	Apparent activation energy/kJ mol ⁻¹
600	13.9
700	16.1
800	16.0
1000	17.9

likely due to the different conditions applied and the intrinsic properties of the prepared Pd catalyst. Furthermore, as far as authors know, these are the first values reported for a real alkaline exchange membrane electrolysis cell. More interestingly, the activation energy hardly varies with the cell potential, indicating that the mechanism for the ethanol electrooxidation is unaltered in the potential range studied. Finally, the slight increase observed in the activation energy with the cell potential may be explained taking into account that at higher potential the dissociative adsorption of ethanol could occur to a larger extent. However, it should always be kept in mind that, according to the results later presented in Table 2, the complete oxidation of the ethanol molecule is almost inappreciable compared to the incomplete oxidation to acetate.

In order to check the influence of ethanol concentration on electro-reforming system performance, a series of linear voltammetry experiments, carried out at 80 °C for different ethanol concentrations, are displayed in Fig. 6. Electrochemical performance shows the most relevant differences in the high current density region (cell voltage range of 0.8–1.3 V), where the least

Table 2

Product distribution (on a molar basis) of the fuel and hydrogen gas streams sampled during the long-terms stability test.

Hydrogen stream			
Gas	Mol %		
H ₂	99.999		
CO ₂	0.001		
Anode side			
	Liquid/mol %		
	Ethanol	Potassium acetate	Potassium carbonate
After 8 h	96.50	3.49	Traces
After 24 h	89.00	10.98	0.02

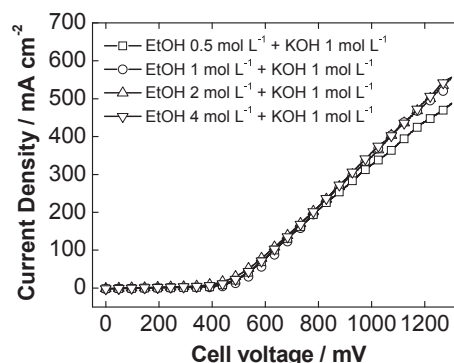


Fig. 6. Influence of the ethanol concentration (Cell temperature of 80 °C and 1 mol L⁻¹ KOH in the fuel composition) on the performance of the electroreforming system.

concentrated fuel feed provides the poorest performance, in agreement with previous studies [4–6,12–15,24,43,44]. Low ethanol concentration (0.5 mol L⁻¹) results in an insufficient fuel supply at high current density, limiting the extension of the electro-catalytic process [13]. However, once ethanol concentration reaches a value of 1 mol L⁻¹, there is no significant effect of this parameter on the high current density region, suggesting an efficient fuel supply to the electrode and a typical region of limitation by ohmic losses. Such a result differs from others where a higher optimum ethanol concentrations (2 mol L⁻¹ or higher) have been found [45–47]. This result can be explained in terms of the enhanced structure/morphology of the developed electrode, more efficient for fuel mass transportation processes compared to conventional electrodes. This point is of great practical interest in terms of both fuel saving and process efficiency.

3.4. Stability study of the system for long working times

In order to test the stability of the sputtered Pd anode, the cell was galvanostatically polarized at 80 °C and a current density of 160 mA cm⁻² for 150 h in 5 consecutive cycles (at the beginning of each cycle of 35 h the anode solution was replaced under open circuit conditions). For each cycle, Fig. 7a presents time evolution of the cell voltage, while Fig. 7b displays the electrical energy consumption at the beginning and at the end of each one to produce 1 Kg of H₂.

As it can be seen, all cycles present a similar behavior with an initial increase in the cell voltage up to approximately 1 V, attained after 15–20 h of operation. The initial increase in the potential can

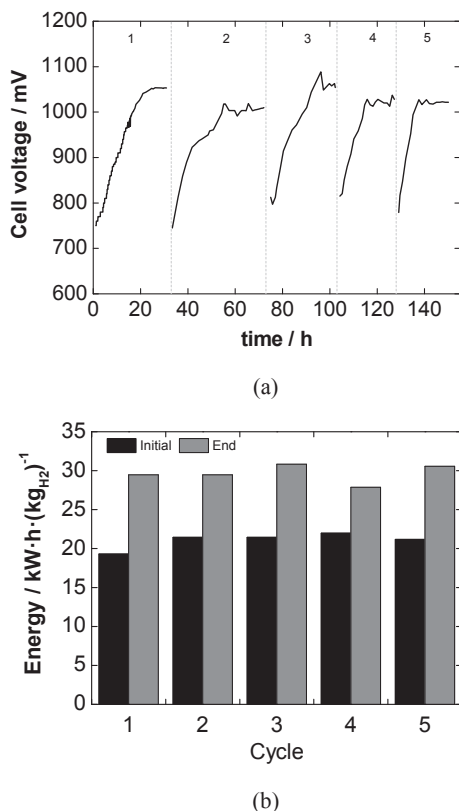


Fig. 7. (a) Evolution of cell voltage with time during cyclic stability test (cell temperature of 80 °C for a 2 mol L⁻¹ ethanol and 1 mol L⁻¹ KOH fuel composition, at a constant current density of 160 mA cm⁻²); (b) Energy consumption of alkaline electro-reforming system for producing H₂ over the cyclic stability test.

be attributed to a catalyst deactivation due to accumulation of intermediate species, which may act as poisoning components for the anodic electrode [48–50]. Once reached that cell voltage, the anode potential is high enough for oxidizing the adsorbates and, hence, regenerating catalytic surface, consequently leading to a more stable cell performance [5]. A reproducible behavior was observed in all cycles based on the obtained potential curves. Further interesting information about the catalyst stability can be extracted from an accelerated stress test (AST) [51]. These tests along with its corresponding conditions have been included on the supporting information material (Fig. A5). The results demonstrated that the Pd electrode is suitably stable under the AST conditions, confirming the good predisposition of this material not only in terms of activity but also in terms of stability. On the other hand, an expected rise in the energy consumption was observed (Fig. 7b) due to the increase in the cell voltage for each operating cycle. Nevertheless, this parameter ranges in all cases between 19 and 30 kWh kg H₂⁻¹. These values are lower than those reported for commercial PEM electrolyzer stacks (50–60 kWh kg H₂⁻¹) [52] or commercial alkaline electrolyzers (48–64 kWh kg H₂⁻¹). Even considering 7.4 kWh kg⁻¹_{EtOH} and 1 kWh kg⁻¹_{electrolyte} as output energy for ethanol and electrolyte respectively [14], the required electrical energy for the electrochemical reforming of ethanol-water solution on the developed system appears a competitive technology, specifically for H₂ production from biomass alcohol streams.

In order to evaluate the catalyst structural stability, a key feature for an electrocatalyst candidate, x-ray diffraction was performed on the fresh and used catalyst, Fig. 8 displays the diffractograms.

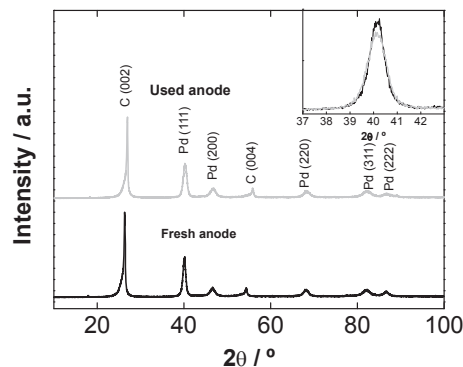
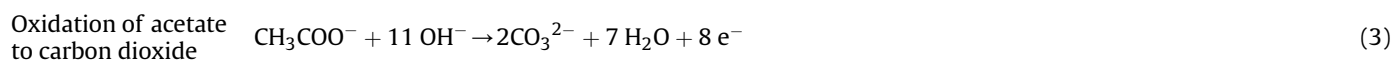
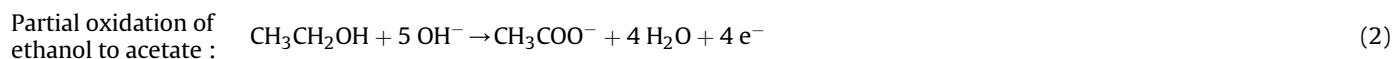


Fig. 8. X-Ray diffractogram of the fresh and used Pd-sputter mesh-like anode. The inset shows a Pd (111) region.

Both show similar feature before and after the stability test. A close view of the (111) diffraction peak of the Pd anodic catalyst is presented on the inset of Fig. 8 in order to analyze in more detail any change of the crystallite size. It can be observed that the diffraction peaks of Pd exhibit almost no change before and after the test, confirming the stability of the sputtered Pd carbon paper under explored alkaline reaction conditions. Furthermore, no metal was detected by Atomic Absorption Spectrophotometry in the fuel solution after more than 200 h of operation, including all performed electrocatalytic experiments. The observed high stability shown by the system can be explained considering that no binder and/or ionomer has been added to the anodic electrode in addition to the good chemical stability of the Pd sputtered anodic catalyst under explored alkaline reaction conditions.

A final priority analysis is the quality of the produced hydrogen. Table 2 collects results from the cathodic gas stream analyzed by gas chromatography. As it can be seen, the purity of the produced hydrogen was 99.999% (H₂ 5.0) with 10 ppm li of CO₂, which is known to act as an inert gas, and which origin might be the carbonates crossover. Despite alkaline conditions of the anodic chamber should lead to the formation of potassium carbonate, the use of water as feed in the cathode favors hydrolysis of the salt and formation of carbon dioxide. Regardless of presence of CO₂ traces, quality of hydrogen is high enough for direct use, for example, in low temperature fuel cells. Moreover, time evolution of the fuel composition (ethanol and detected products such as potassium acetate and carbonate) is also collected in Table 2.

Potassium acetate is almost the sole electrooxidation product, with traces of potassium carbonate. It indicates that partial oxidation involving 4 electrons from ethanol to acetate (Eq. (2)) is favored when Pd is used as electrocatalyst vs. its further oxidation to carbonates (Eq. (3)) [53]. At this point, it is also interesting to note that potassium acetate is a product that finds application as a catalyst for the polymer industry, as a food additive and in medicine and biochemistry [54–56]. Furthermore, the intrinsic selectivity of Pd for producing mainly potassium acetate could be considered advantageous since it would facilitate subsequent purification steps. It is also of great practical interest compared to other explored electrocatalytic systems, e.g., based on ethyleneglycol or glycerol, where a complex mixture of oxidation products is obtained [24,57–61]. Nonetheless, some important advances have been achieved on improving the selectivity to these polyalcohols when a second metal is added, such as demonstrated by Simões et al. [62,63] and Zalinee et al. [64,65], mainly by the introduction of Bi in the catalyst formulation and by the synthesis of advanced catalytic structure such as self-supported Pd_xBi catalysts.



In summary, this paper has presented an alternative procedure for preparing Pd by sputtering, rendering to a self-supported Pd mesh catalyst which effectively produces hydrogen from the alkaline ethanol electrooxidation. Besides the promising results, there is room for improvements based on opportunities that the system offers. One challenge is the reduction of the palladium loading in the catalyst maintaining the good performance, key factor considering that Pd is more affordable than Pt. For this, it will be necessary to reduce the size of the “Pd walls” formed during the sputtering without modifying the structure and, more importantly, the catalytic properties. This demands an effort in order to optimize the sputtering process, which is actually the challenge for future works.

4. Conclusions

A novel Pd self-standing architecture electrode has been prepared onto a carbon microfiber paper by using magnetron sputtering technique. This leads to continuous Pd mesh-like structure containing large pores and suitable porosity of around 30% for electro-catalytic applications. Obtained Pd anode shows a high electro-catalytic performance (up to 700 mA cm^{-2}), corresponding to high very pure (99.999%) H_2 production rates (in agreement with those predicted by Faraday's law) and with a lower energy demand than alkaline water electrolysis systems. Such behavior can be attributed to the particular mesh-like structure of the Pd anode, where most of the active layer is on the uppermost layer of the carbon paper in contact with the membrane, maintaining most of the macroporous structure of the carbon paper. KOH is the most effective electrolyte in the fuel solution, which in combination with a 1 mol L^{-1} ethanol solution leads to the most adequate fuel composition without any mass transport limitation. Temperature exerts the expected beneficial effect with an increase in the performance up to 90°C . The proposed system has demonstrated to be stable for 150 h operating in 5 successive cycles, with a slight increase in the potential during first hours until stabilization. This behavior has been repeatedly observed along the cycles. The excellent chemical stability of the Pd anodic electrode under the explored alkaline conditions (checked by XRD and Atomic Absorption spectrophotometry) and the absence of ionomer/binder in the catalytic layer are responsible for the observed high stability of the system. Finally, potassium acetate has been detected as the main anodic product resulting from the partial electro-oxidation of ethanol under alkaline media in the sputtered Pd mesh-like anode.

Acknowledgements

José J. Linares would like to thank the Conselho Nacional de Desenvolvimento Científico e Tecnológico (CNPq) for the financial support through the Universal Call (Project no. 474381/2013-7).

Appendix A. Supplementary data

Supplementary data related to this article can be found at <http://dx.doi.org/10.1016/j.jpowsour.2016.05.004>.

References

- [1] M. Momirlan, T.N. Veziroglu, *Renew. Sust. Energy Rev.* 6 (2002) 141–179.
- [2] A. Nieto-Márquez, D. Sánchez, A. Miranda-Dahdal, F. Dorado, A. De Lucas-Consuegra, J.L. Valverde, *Chem. Eng. Process.* 74 (2013) 14–18.
- [3] H. Takenaka, E. Torikai, Y. Kawami, N. Wakabayashi, *Int. J. Hydrogen Energy* 7 (1982) 397–403.
- [4] T. Take, K. Tsurutani, M. Umeda, *J. Power Sources* 164 (2007) 9–16.
- [5] A. Caravaca, F.M. Sapountzi, A. De Lucas-Consuegra, C. Molina-Mora, F. Dorado, J.L. Valverde, *Int. J. Hydrogen Energy* 37 (2012) 9504–9513.
- [6] G. Sasikumar, A. Muthumeenal, S.S. Pethaiah, N. Nachiappan, R. Balaji, *Int. J. Hydrogen Energy* 33 (2008) 5905–5910.
- [7] C.R. Cloutier, D.P. Wilkinson, *Int. J. Hydrogen Energy* 35 (2010) 3967–3984.
- [8] Z. Hu, M. Wu, Z. Wei, S. Song, P.K. Shen, *J. Power Sources* 166 (2007) 458–461.
- [9] A.T. Marshall, R.G. Haverkamp, *Int. J. Hydrogen Energy* 33 (2008) 4649–4654.
- [10] S. Kongjao, S. Damronglerd, M. Hunsom, *J. Appl. Electrochem.* 41 (2011) 215–222.
- [11] J. De Paula, D. Nascimento, J.J. Linares, *Chem. Eng. Trans.* (2014) 205–210.
- [12] C. Lamy, T. Jaubert, S. Baranton, C. Coutanceau, *J. Power Sources* 245 (2014) 927–936.
- [13] A. Caravaca, A. De Lucas-Consuegra, A.B. Calcerrada, J. Lobato, J.L. Valverde, F. Dorado, *Appl. Catal. B* 134–135 (2013) 302–309.
- [14] Y.X. Chen, A. Lavacchi, H.A. Miller, M. Bevilacqua, J. Filippi, M. Innocenti, A. Marchionni, W. Oberhauser, L. Wang, F. Vizza, *Nat. Commun.* 5 (2014) 4036.
- [15] A. De Lucas-Consuegra, A.B. Calcerrada, A.R. De La Osa, J.L. Valverde, *Fuel Process. Technol.* 127 (2014) 13–19.
- [16] H. Xu, W.A. Goedel, *Small* 1 (2005) 808–812.
- [17] S. Press, *Sculptured Thin Films, Nanoengineered Morphology and Optics*, Washington, 2005.
- [18] D. Horwat, J.F. Pierson, A. Billard, *Surf. Coat. Technol.* 201 (2007) 7060–7065.
- [19] X. Zhang, J. Hampshire, K. Cooke, X. Li, D. Pletcher, S. Wright, K. Hyde, *Int. J. Hydrogen Energy* 40 (2015) 2452–2459.
- [20] K.J. Bryden, J.Y. Ying, *Mater. Sci. Eng. A* 204 (1995) 140–145.
- [21] Y. Leng, G. Chen, A.J. Mendoza, T.B. Tighe, M.A. Hickner, C.-Y. Wang, *J. Am. Chem. Soc.* 134 (2012) 9054–9057.
- [22] A.P. Nascimento, J.J. Linares, *J. Braz. Chem. Soc.* 25 (2014) 509–516.
- [23] C.A. Angelucci, H. Varela, G. Tremiliosi-Filho, J.F. Gomes, *Electrochim. Commun.* 33 (2013) 10–13.
- [24] J. De Paula, D. Nascimento, J.J. Linares, *Chem. Eng. Trans.* (2014) 205–210.
- [25] A.N. Geraldes, D.F. da Silva, E.S. Pino, J.C.M. da Silva, R.F.B. de Souza, P. Hammer, E.V. Spinacé, A.O. Neto, M. Linardi, M.C. dos Santos, *Electrochim. Acta* 111 (2013) 455–465.
- [26] J.J.L. Joanna de Paula, Deborah Nascimento, *J. Appl. Electrochem.* 45 (7) (2015) 689–700.
- [27] M.Z.F. Kamarudin, S.K. Kamarudin, M.S. Masdar, W.R.W. Daud, *Int. J. Hydrogen Energy* 38 (2013) 9438–9453.
- [28] L. Wang, M. Bevilacqua, Y.-X. Chen, J. Filippi, M. Innocenti, A. Lavacchi, A. Marchionni, H. Miller, F. Vizza, *J. Power Sources* 242 (2013) 872–876.
- [29] D. Strmcnik, K. Kodama, D. van der Vliet, J. Greeley, V.R. Stamenkovic, N.M. Marković, *Nat. Chem.* 1 (2009) 466–472.
- [30] E. Sitta, B.C. Batista, H. Varela, *Chem. Commun.* 47 (2011) 3775–3777.
- [31] I. Katsounaros, K.J.J. Mayrhofer, *Chem. Commun.* 48 (2012) 6660–6662.
- [32] J. Durst, M. Chatenet, F. Maillard, *PCCP* 14 (2012) 13000–13009.
- [33] D. Strmcnik, D.F. van der Vliet, K.C. Chang, V. Komanicky, K. Kodama, H. You, V.R. Stamenkovic, N.M. Marković, *J. Phys. Chem. Lett.* 2 (2011) 2733–2736.
- [34] M. Miller, A. Bazylak, *J. Power Sources* 196 (2011) 601–613.
- [35] D. Wang, J. Liu, Z. Wu, J. Zhang, Y. Su, Z. Liu, C. Xu, *Int. J. Electrochem. Sci.* 4 (2009) 1672–1678.
- [36] M. Wang, Z. Wang, X. Gong, Z. Guo, *Renew. Sust. Energy Rev.* 29 (2014) 573–588.
- [37] B. Pierozynski, T. Mikolajczyk, M. Turemko, E. Czerwosz, M. Kozłowski, *Int. J. Hydrogen Energy* 40 (2015) 1795–1799.
- [38] A. Dutta, J. Datta, *Int. J. Hydrogen Energy* 38 (2013) 7789–7800.
- [39] L.V. Kumar, S. Addo Ntim, O. Sae-Khow, C. Janardhana, V. Lakshminarayanan, S. Mitra, *Electrochim. Acta* 83 (2012) 40–46.
- [40] L. Ma, D. Chu, R. Chen, *Int. J. Hydrogen Energy* 37 (2012) 11185–11194.
- [41] S. Sun, Z. Jusys, R.J. Behm, *J. Power Sources* 231 (2013) 122–133.
- [42] P. Wang, X. Lin, B. Yang, J.-M. Jin, C. Hardacre, N.-F. Yu, S.-G. Sun, W.-F. Lin, *Electrochim. Acta* 162 (2015) 290–299.
- [43] S. Uhm, H. Jeon, T.J. Kim, J. Lee, *J. Power Sources* 198 (2012) 218–222.
- [44] S. Tuomi, A. Santasalo-Aarnio, P. Kanninen, T. Kallio, *J. Power Sources* 229

- (2013) 32–35.
- [45] T.S. Zhao, Y.S. Li, S.Y. Shen, *Front. Energy Power Eng. China* 4 (2010) 443–458.
- [46] L. An, T.S. Zhao, *Int. J. Hydrogen Energy* 36 (2011) 9994–9999.
- [47] Y.S. Li, Y.L. He, W.W. Yang, *Int. J. Hydrogen Energy* 38 (2013) 13427–13433.
- [48] J. Datta, A. Dutta, S. Mukherjee, *J. Phys. Chem. C* 115 (2011) 15324–15334.
- [49] A. Dutta, S.S. Mahapatra, J. Datta, *Int. J. Hydrogen Energy* 36 (2011) 14898–14906.
- [50] D. Basu, S. Basu, *Int. J. Hydrogen Energy* 37 (2012) 4678–4684.
- [51] S. Zhang, X.-Z. Yuan, J.N.C. Hin, H. Wang, K.A. Friedrich, M. Schulze, *J. Power Sources* 194 (2009) 588–600.
- [52] M. Carmo, D.L. Fritz, J. Mergel, D. Stolten, *Int. J. Hydrogen Energy* 38 (2013) 4901–4934.
- [53] S.Y. Shen, T.S. Zhao, Q.X. Wu, *Int. J. Hydrogen Energy* 37 (2012) 575–582.
- [54] H. Cheung, R.S. Tanke, G.P. Torrence, *Acetic Acid*, *Ullmann's Encyclopedia of Industrial Chemistry*, Wiley-VCH Verlag GmbH & Co. KGaA, 2000.
- [55] <http://www.food.gov.uk/science/additives/enumberlist>, in, 2014.
- [56] D. Ulmer, *J. Int. Soc. Plast.* 8 (1994) 7–10.
- [57] Z. Zhang, L. Xin, Z. Wang, W. Li, in: *AIChE 2012–2012 AIChE Annual Meeting, Conference Proceedings*, 2012.
- [58] A.N. Gerales, D.F. Silva, J.C.M. Silva, R.F.B. Souza, E.V. Spinacé, A.O. Neto, M. Linardi, M.C. Santos, *J. Braz. Chem. Soc.* 25 (2014) 831–840.
- [59] T. Matsumoto, M. Sadakiyo, M.L. Ooi, S. Kitano, T. Yamamoto, S. Matsumura, K. Kato, T. Takeguchi, M. Yamauchi, *Sci. Rep.* 4 (2014) 5620.
- [60] L. Demarconnay, S. Brimaud, C. Coutanceau, J.M. Léger, *J. Electroanal. Chem.* 601 (2007) 169–180.
- [61] L. Xin, Z. Zhang, J. Qi, D. Chadderdon, W. Li, *Appl. Catal. B* 125 (2012) 85–94.
- [62] M. Simões, S. Baranton, C. Coutanceau, *Appl. Catal. B* 110 (2011) 40–49.
- [63] M. Simões, S. Baranton, C. Coutanceau, *ChemSusChem* 5 (2012) 2106–2124.
- [64] A. Zalineeva, A. Serov, M. Padilla, U. Martinez, K. Artyushkova, S. Baranton, C. Coutanceau, P.B. Atanassov, *J. Am. Chem. Soc.* 136 (2014) 3937–3945.
- [65] A. Zalineeva, S. Baranton, C. Coutanceau, *Electrochim. Acta* 176 (2015) 705–717.